

Unsaturated polyester nanocomposites filled with nano alumina

R. Baskaran · M. Sarojadevi · C. T. Vijayakumar

Received: 2 December 2010 / Accepted: 12 February 2011 / Published online: 25 February 2011
© Springer Science+Business Media, LLC 2011

Abstract Alumina nanoparticles (60–70 nm) were prepared by the sol–gel technique using citric acid and aluminum nitrate. Casting technique was used to make nanocomposites of unsaturated polyester (UPR) and nano alumina. Transmission Electron Microscopy (TEM) study demonstrated that nano alumina particles were dispersed uniformly in the UPR matrix and agglomeration of particles was found at higher filler loading (>5 wt%). The nanocomposites show higher tensile, flexural and impact strength than pristine UPR. Scanning Electron Microscopy (SEM) of the fractured surface of tensile test samples show that the ductile fracture of UPR was converted to brittle fracture with the addition of nano alumina. Dynamic Mechanical Analysis (DMA) studies showed the storage modulus increased up to 5 wt% loading of nano alumina. The impact strength and storage modulus results agree well. The thermogravimetric studies revealed that the nanocomposites were having higher thermal stability than the pure UPR. As the concentration of the nano alumina in the UP resin increased, the char yield was also increased.

Introduction

Polymer nanocomposites comprise a new class of materials in which nanoscale particulates (e.g., clay or other inorganic minerals) are finely dispersed within the matrices and intensive research efforts have been devoted to the development of nanocomposites [1–11]. It is known that the mechanical properties of the composites are, in general, strongly related to the aspect ratio of the filler particles. The mechanical properties of the composites filled with micron sized filler particles are inferior to those filled with nanoparticles of the same filler [12–14]. In addition, the physical properties, such as surface smoothness and barrier properties cannot be achieved by using conventional micron sized particles. An important review article by Kopczynska et al. [15, 16] concludes that properties of composites are decided by the interfaces between matrices and nano particulates. Layered silicates, such as montmorillonite, which has a fairly large aspect ratio, have been extensively studied [1–4]. In spite of many attractive improvements in physical and mechanical properties of the polymer/intercalated or exfoliated) clay nanocomposites, a dramatic decrease in toughness due to the addition of clay has been reported.

Other nanoparticles, such as alumina, silica [5, 6, 17], zinc oxide [18, 19], calcium carbonate [7–10], carbon black [20], carbon nanotubes [21–23], gold [24], or other metals [25] have been used to prepare nanocomposites. Among them, alumina is the most cost effective and widely used material in the family of engineering ceramics. But its use as a nanomaterial for reinforcement is limited. Incorporation of nano alumina improves properties like hardness, wear resistance, dielectric properties, resists strong acid, and alkali attack at elevated temperatures, good thermal conductivity, size and shape capability, high strength and

R. Baskaran · C. T. Vijayakumar (✉)
Department of Polymer Technology, Kamaraj College
of Engineering and Technology, S.P.G.C. Nagar, K. Vellakulam
Post, Madurai 625 701, Tamil Nadu, India
e-mail: ctvijay22@yahoo.com

M. Sarojadevi
Department of Chemistry, Anna University,
Chennai 600 025, Tamil Nadu, India

stiffness, etc. With this reasonably good combination of properties and an attractive price, nano alumina filled composites has a very wide range of applications [26, 27].

Unsaturated polyester resins (UPRs) are one of the most widely used thermosetting materials because they are relatively inexpensive and offer advantage such as being light in weight and possessing reasonably good mechanical properties. Unsaturated polyester resin have a leading role in the development of fibreglass reinforced products, having tremendous versatility and low cost. The use of UPRs in bulk and sheet molding compounds results in composite materials that have high strength, dimension stability, and very good surface qualities [28–34]. They have many applications in automotive, aircraft, electrical, and appliance components as substitutes for traditional materials.

The objective of the study is to enhance the performance of polymer nanocomposites by using unsaturated polyester (UPR) and nano alumina. The nano alumina particles were synthesized by sol–gel process and characterized. Nanocomposites were fabricated by reinforcing alumina particles in UPR matrix and their mechanical, thermal as well as failure mechanism as a function of nano alumina concentration in the UPR matrix were evaluated and discussed.

Experimental

Materials

Analytical grade citric acid and aluminum nitrate, procured from Merck Chemicals Limited, Mumbai, India were used as raw materials to prepare the nanosized alumina. The general purpose unsaturated polyester resin, cobalt naphthenate (accelerator), and methyl ethyl ketone peroxide (catalyst) were procured from GVS Agencies, Madurai, India.

Synthesis of nano alumina

The nano-sized alumina was synthesized by sol–gel technique. Aluminum nitrate (158 g) and citric acid (105 g) were dissolved in 100 mL of water. The aluminum nitrate and citric acid solution was digested for 4 h at 80 °C and stirred constantly. Viscosity and color were changed as the solution turned into a transparent gel. The gel was calcined at 1,000 °C for 2 h in muffle furnace to get nano alumina powder.

Preparation of nanocomposites

Unsaturated polyester resin (400 mL) was taken in a container. Nano alumina of definite quantity (1, 3, 5, 7, and 9 wt%) was added to produce nano alumina dispersed

polyester mix. It was stirred well using a mechanical stirrer at 2,000 rpm for 45 min to produce nanocomposite gel coat system. Methyl ethyl ketone peroxide catalyst (4 mL) and cobalt napthanate accelerator (1 mL) were added to the mixture to initiate the curing reaction. Sheets of size 350 × 350 × 3 mm³ were cast in a glass mold and allowed to cure for 24 h at room temperature followed by post curing at 70 °C for 3 h.

Characterization and testing

Transmission electron microscopy

Particle size of nano alumina and nano alumina dispersed in UPR matrix were characterized using JEOL JEM 1200EX electron microscope.

FT-IR

The materials were characterized by FT-IR measurements and were performed in a Shimadzu 8400S series FT-IR spectrophotometer with 2 cm⁻¹ resolution. The KBr pellet technique was used to record the FT-IR spectrum.

Mechanical properties

Tensile test specimens were prepared according to ASTM D 638 and the tests were performed at room temperature using Instron 4301 Universal Testing Machine (UTM) with crosshead speed of 5 mm min⁻¹. Flexural properties were evaluated using Instron 4301 UTM as per ASTM D 790 standard. Izod impact strength was determined using Frank impact testing machine following ASTM D-256 standard.

Scanning electron microscopy

Mechanically fractured tensile samples were analyzed using S-3400 scanning electron microscope (SEM).

Thermal properties

Dynamic mechanical analysis (DMA) [35] was performed using Netzsch (DMA 242C) dynamic mechanical analyzer in the three-point bending mode at a frequency of 10 Hz and amplitude of 120 μm over the temperature range of 20–180 °C at a heating rate of 2 °C min⁻¹. Thermogravimetric analysis (TGA) was carried out using Netzsch STA 409PC thermogravimetric analyzer. Samples were ground to fine powder and placed in alumina sample pan. All samples were heated in nitrogen atmosphere at a heating rate of 10 °C min⁻¹ from ambient to 800 °C.

Result and discussion

Transmission electron microscopy

A typical TEM micrograph of synthesized alumina particles is shown in Fig. 1a. Alumina particles are spherical and most of them were dispersed in the primary particle form with a diameter of about 60–70 nm. Figure 1b, c is TEM micrographs of UPR/alumina nanocomposites with nano alumina 5 and 7 wt%, respectively. For 5 wt% alumina nanocomposite, a good dispersion is achieved. Most of the alumina particles are uniformly distributed as nanosized particles in the UPR matrix. The particles appear to be agglomeration free and the individual particles can be identified very clearly.

However, more aggregates are found in the UPR/alumina nanocomposite with 7 wt% of alumina nanoparticles, which suggests a poor dispersion. The poor dispersion may be due to the interaction between particles leading to agglomeration. This is reasonable, considering that at high nano alumina concentration, the inter particle distance is small, and hence, flocculation of these nanoparticles can occur [36].

FT-IR

The structure of nanocomposites was studied using FT-IR spectroscopy and the results are shown in Fig. 2. Pure UPR shows the characteristic peaks at $2,985\text{ cm}^{-1}$ (C–H stretching vibration), $1,720\text{--}1,730\text{ cm}^{-1}$ (C=O stretching vibrations), $1,443\text{ cm}^{-1}$ (C=C stretching vibrations), $1,182$ and $1,263\text{ cm}^{-1}$ (CH_2 wagging and scissoring) and 750 and 705 cm^{-1} (out of plane ring bending vibrations). The nano alumina shows the characteristic peak at 1411, 1635, 2385, and 3348 cm^{-1} (shows the existence of water molecules that were entrapped in the nano alumina) [37]. The composites show a characteristic peaks at $2,940\text{ cm}^{-1}$ (C–H stretching vibrations), $1,725\text{ cm}^{-1}$ (C=O stretching vibrations),

$1,635\text{ cm}^{-1}$, $1,443$ (C=C stretching vibrations), $1,182$ and $1,263\text{ cm}^{-1}$ (CH_2 wagging and scissoring), and 750 and 705 cm^{-1} (out of plane ring bending vibrations). The differences noted in the regions $1,500\text{--}1,000$ and $3,000\text{ cm}^{-1}$ among the spectra of pure UPR, pure nano alumina, and UPR/nano alumina indicate polymer–alumina interactions.

Mechanical properties

The tensile strength of UPR/nano alumina with different filler content is given in Fig. 3. Pure UPR shows tensile strength of 58 MPa. Tensile strength of nano alumina-filled UPR are 61, 64, 66, 62, and 60 MPa for 1, 3, 5, 7, and 9 wt% nano alumina-loaded UPR, respectively. Unsaturated polyester with 5 wt% of nano alumina shows maximum increase in strength, and on further addition of nano alumina (>5 wt%) the tensile strength decreases. Tensile strength of nanocomposites is enhanced when the interfacial adhesion is improved. This result can be ascribed to better stress transfer at the interface between matrix and nano alumina. The improvement of interfacial adhesion can prevent dewetting at the UPR/nano alumina interface during tensile deformation. Therefore, well adhering nano alumina can bear part of the load applied to the matrix and contribute to the tensile strength of the nanocomposites [38–40]. For higher loading of nano alumina in the resin matrix, nanosized-particle agglomeration is easier. Since the agglomerated particles generate defects in the material, stress concentration is likely to occur within the resin or agglomerated particles will generate slippage within the material due to external force, resulting in decreased tensile properties [41].

The results of flexural strength of the composite system as a function of nano alumina filler loading are presented in Fig. 4. Flexural strength of pure UPR matrix is 98 MPa. The graph shows an increasing trend as the filler loading increases up to 5 wt% (109 MPa). However, slight decrease in flexural strength is observed at 7 wt% alumina

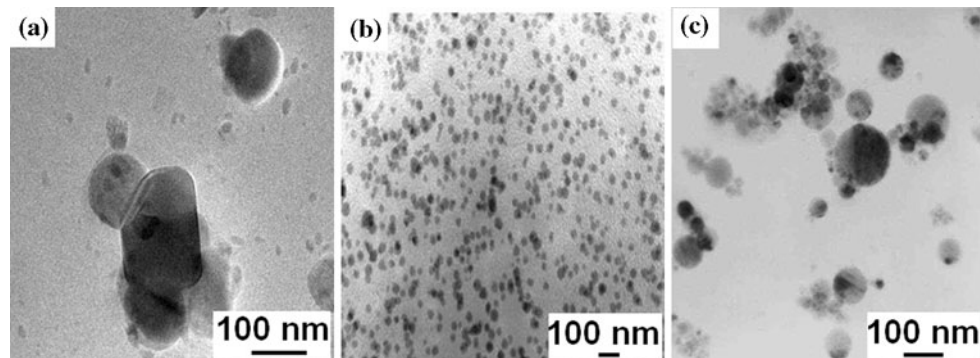


Fig. 1 TEM image of **a** Alumina nanoparticles, **b** UPR/5 wt% nano alumina, and **c** UPR/7 wt% nano alumina

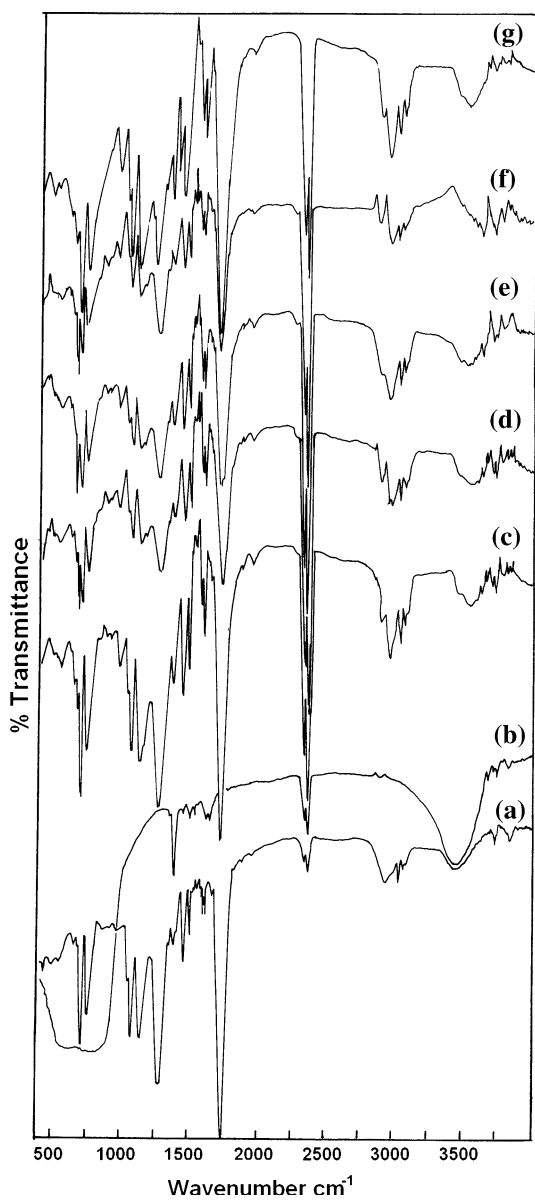


Fig. 2 FTIR spectra of pure UPR, nano alumina and UPR/alumina nanocomposites **(a)** Pure polyester **(b)** Nano alumina **(c)** UPR/1% nano alumina **(d)** UPR/3% nano alumina **(e)** UPR/5% nano alumina **(f)** UPR/7% nano alumina **(g)** UPR/ 9% nano alumina

(105 MPa). High aspect ratio provides high surface area, hence results in more contact area between the filler and the matrix. Therefore, by presumably good adhesion and bonding existing between the filler and matrix, positive reinforcement effect occurs in alumina-filled UPR which might increase the strength of the composites. The effective bonding between inorganic fillers and matrix components typically improved the flexural strength of polymer composites. The agglomerations of alumina results in inhomogeneous distribution and hence weaken the interaction between the filler and matrix. This subsequently reduces the flexural strength of alumina composite system [42].

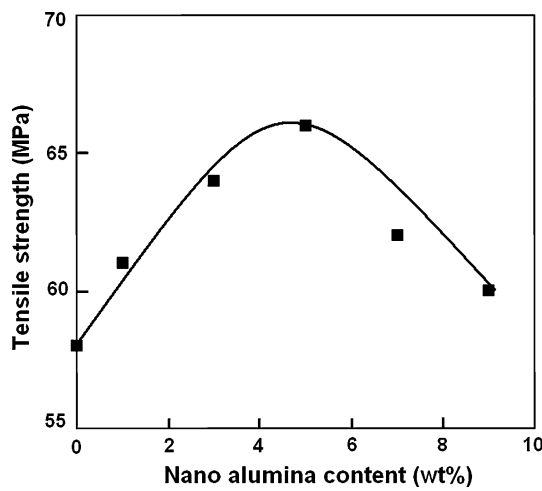


Fig. 3 Effect of alumina nanoparticle content on the tensile strength of unsaturated polyester

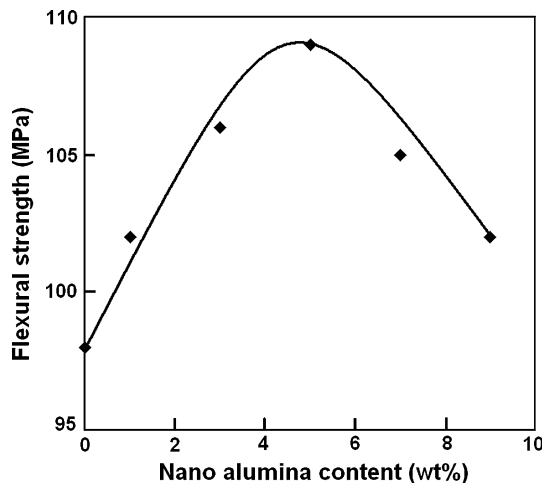


Fig. 4 Effect of alumina nanoparticle content on the flexural strength of unsaturated polyester

The relationship of nano alumina content and impact strength of UPR/alumina nanocomposites is shown in Fig. 5. Pure UPR shows impact strength of 20 J m^{-1} . When the nano alumina content is 5 wt% the impact strength of nanocomposites increases (32 J m^{-1}) to a maximum and then decreases with further addition of nano alumina. UPR with 7 wt% nano alumina shows impact strength of 29 J m^{-1} . This variation of impact strength can be attributed to two things. First when nano alumina content is <5 wt% there is seldom agglomerated nano alumina in the matrix. The presence of fine particles dispersed within the matrix makes plastic deformation easier. Therefore, during the fracture of a composite in which the nanoparticle is well dispersed, the stress will have to be bigger to start the micro crack in the UPR matrix, and the impact energy will largely be absorbed by the exhibited plastic deformation, which occurs more easily around the nanoparticles. Hence,

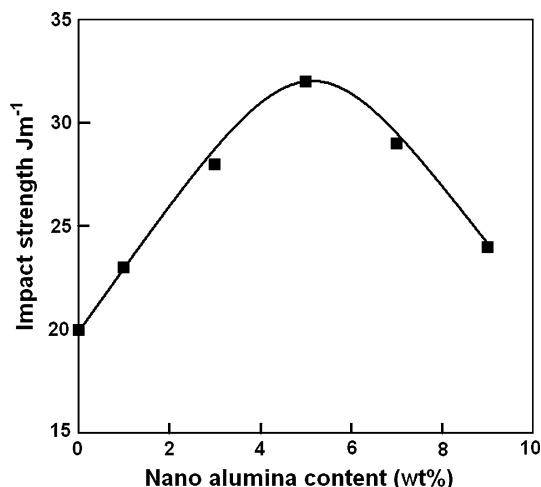


Fig. 5 Effect of alumina nanoparticle content on the impact strength of unsaturated polyester

the good nano alumina dispersion resulting in less agglomeration leads to a better impact strength of the nanocomposites [43]. The second reason for the variation in the impact strength is that when nano alumina content is >5 wt%, it easily agglomerates into large aggregated particles, which will become the site of stress concentration and can act as a micro crack initiator. Therefore, a larger aggregate is a weak point that lowers the stress required for the composite to fracture and hence the impact strength of the nanocomposites would be decreased [39, 44, 45].

Fracture analysis

The SEM pictures of tensile fractured surfaces of UPR/alumina nanocomposites are given in Fig. 6. The possible origins of crack initiation in a composite material are air bubble or voids, resin-rich area, foreign matter such as dust particles, particle size and poor particle matrix adhesion [46]. The fractured surface of the unfilled resin (Fig. 6a) shows a brittle failure. At low levels of nano alumina in UPR, good adhesion between the particle and polymer matrix can be seen from the fact that there is not much

particle pull out and subsequent cavity formation (Fig. 6b). Another possible mode of failure (Fig. 6c) is noted in nanocomposites wherein agglomeration of the nano alumina particles is seen. Since the nano alumina particles are randomly oriented, large numbers of them are subjected to tensile stresses acting perpendicular to the plane and crack propagation occurs parallel to the plane. It is clearly seen in UPR/7 wt% nano alumina sample (Fig. 6c) have experienced a high level of debonding and particle pull out.

Dynamic mechanical analysis

The $\tan \delta$ for pristine polyester and alumina nanocomposites are measured as the function of temperature (Fig. 7). On addition of nano alumina particle in the matrix the $\tan \delta$ peak shifts to higher temperature, which suggests that there is an increase in T_g . The T_g increased from 93 to

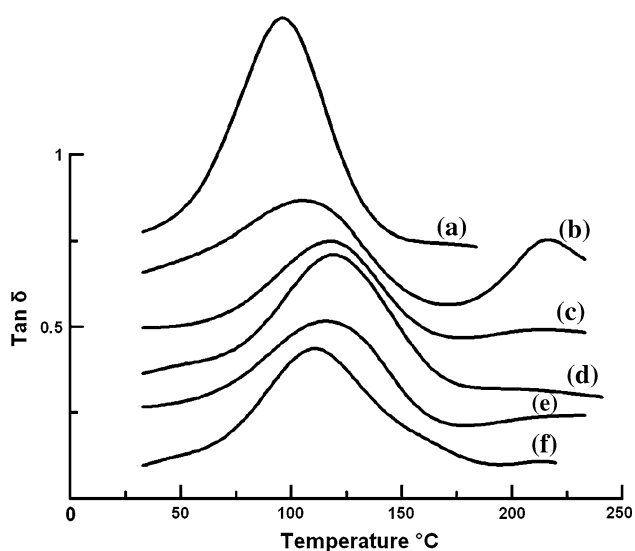


Fig. 7 Temperature dependence of $\tan \delta$ of UPR/alumina nanocomposites. (a) Pure polyester, (b) UPR/1% nano alumina, (c) UPR/3% nano alumina, (d) UPR/5% nano alumina, (e) UPR/7% nano alumina, (f) UPR/9% nano alumina. Data are offset for clarity but not otherwise scaled

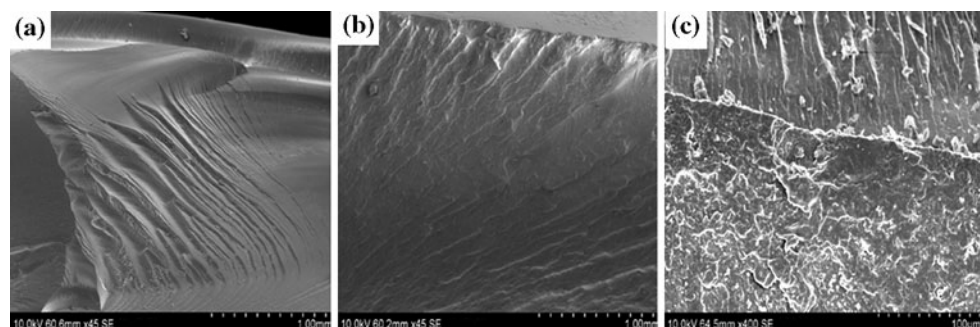


Fig. 6 SEM image of **a** pure polyester, **b** UPR/5 wt% nano alumina, and **c** UPR/7 wt% nano alumina

120 °C after addition of 5 wt% nano alumina. On further addition of nano alumina (>5 wt%) T_g decreases continuously. It decreases to 117 and 111 °C for 7 and 9 wt% of nano alumina, respectively. Since the glass transition process is related to the molecular motion, the T_g is considered to be affected by molecular packing, chain rigidity, and linearity [47]. The increase in T_g may be attributed to maximizing the adhesion between polymer and nano alumina particles. Because of the nanometer size which restricts segmental motion near the organic–inorganic interface, which is a typical effect for the inclusion of nano alumina in the polymer system [48, 49]. The existence of agglomeration of particles in the matrix (>5 wt%) possibly decreases the T_g at higher nano alumina content. The agglomerated zone is a weak zone due to weak interface bonding between matrix and particles, which causes low T_g values.

The effect of nano alumina on storage modulus of unsaturated polyester is shown in Fig. 8. The storage modulus of the UPR/alumina nanocomposites increases up to 5 wt% nano alumina content in unsaturated polyester matrix. Pure polyester shows storage modulus of 6,787 MPa. Unsaturated polyester with 5 wt% of nano alumina shows maximum value of 10,233 MPa, which is 51% higher than pure unsaturated polyester matrix. It confirms that well-dispersed alumina nanoparticles stiffen the polyester matrix [50]. However, when the nanoparticle content is increased (>5 wt%) the stiffening effect is progressively reduced with increasing temperature most probably due to agglomeration of alumina nanoparticles [51]. For unsaturated polyester with 9 wt% nano alumina, storage modulus is 8,106 MPa. However, the rate of decrease of storage modulus in nano alumina-filled unsaturated polyester is low.

Since storage modulus is inversely proportional to brittleness [52], this implies that brittleness goes down in the same concentration interval and after a minimum at 5 wt% alumina, it goes up again. It has been demonstrated that

high brittleness corresponds to low impact strength and vice versa; an equation connecting these two parameters has been derived [53]. Thus, impact strength results displayed in Fig. 5 (maximum at 5 wt% alumina) agree with the storage modulus results (Fig. 8).

Thermogravimetric analysis

The TGA curves of pure UPR and its nanocomposites with different compositions of nano alumina are shown in Fig. 9. The onset temperature, end temperature, and degradation temperatures at 10% weight loss values obtained from the TGA data of pure UPR and UPR/alumina

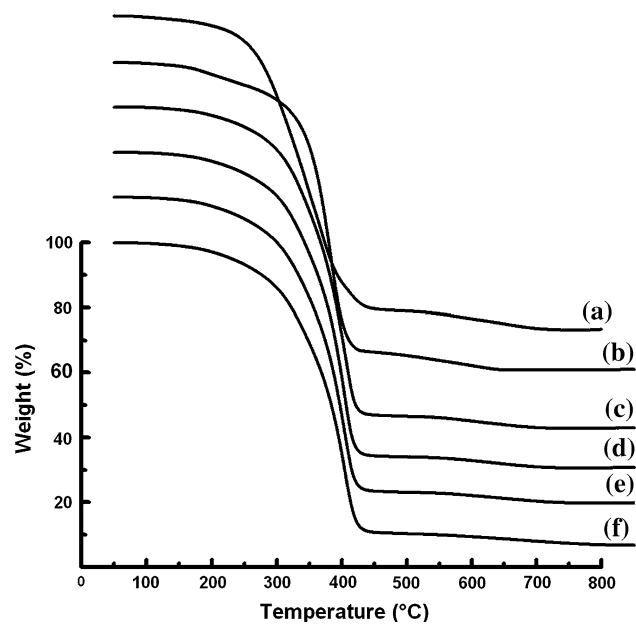


Fig. 9 TGA thermo grams of UPR/alumina nanocomposites. (a) Pure polyester, (b) UPR/1% nano alumina, (c) UPR/3% nano alumina, (d) UPR/5% nano alumina, (e) UPR/7% nano alumina, (f) UPR/9% nano alumina. Data are offset for clarity but not otherwise scaled

Fig. 8 Temperature dependence of storage modulus of UPR/alumina nanocomposites. (a) Pure polyester, (b) UPR/1% nano alumina, (c) UPR/3% nano alumina, (d) UPR/5% nano alumina, (e) UPR/7% nano alumina, (f) UPR/9% nano alumina. Data are offset for clarity but not otherwise scaled

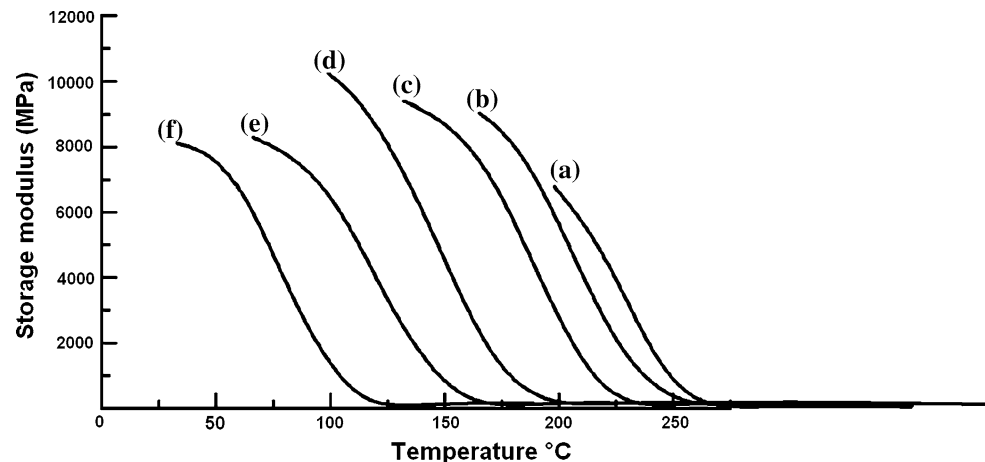


Table 1 TGA data of pure UPR and UPR/alumina nanocomposites

| Composition | Onset temp(°C) | End temp(°C) | T _{max} (°C) | T _{10%} (°C) | Weight residue (%) |
|------------------------|----------------|--------------|-----------------------|-----------------------|--------------------|
| Unfilled UPR | 165 | 422 | 344 | 263 | 3.0 |
| UPR/1 wt% Nano alumina | 168 | 425 | 376 | 279 | 4.9 |
| UPR/3 wt% Nano alumina | 168 | 430 | 379 | 283 | 1.0 |
| UPR/5 wt% Nano alumina | 170 | 433 | 381 | 285 | 2.8 |
| UPR/7 wt% Nano alumina | 173 | 436 | 383 | 286 | 5.8 |
| UPR/9 wt% Nano alumina | 178 | 438 | 385 | 289 | 6.7 |

nanocomposites are given in Table 1, which indicates that the thermal stability of the pure UPR was enhanced by the incorporation of alumina particles. For pure UPR, the maximum degradation temperature is 344 °C, while for the composites it increases to 376, 379, 381, 383, and 385 °C for 1, 3, 5, 7, and 9 wt% of nano alumina in UPR/alumina nanocomposites, respectively. In all cases, a single step degradation occurs. Therefore, the incorporation of the nano alumina resulted in pronounced improvement in thermal stability. This can be attributed to the homogeneous distribution of nano alumina particles as well as the tortuous path in the composites that hinders diffusion of the volatile decomposition products in the composites compared to that in pure UPR [54].

Conclusions

The nanosized alumina was prepared through sol-gel technique using citric acid and aluminum nitrate. TEM study showed that the synthesized alumina was of nanosize and nanoparticles were distributed in the UPR matrix uniformly and particle agglomeration was found at above 5 wt% nano alumina. The nanocomposites show slightly higher tensile, flexural, and impact strength than pristine UPR. The fracture surface of tensile test samples were also examined through SEM and show that ductile fracture of UPR is converted into brittle fracture with addition of alumina. The dynamic mechanical measurements showed that glass transition temperature and storage modulus of the pristine UPR increased upon addition of nano alumina particles up to a level of 5 wt%. The presence of nano alumina in UPR improves the thermal stability of the system as evidenced by thermogravimetric analysis.

References

1. Kim GM, Lee DH, Hoffmann B, Kressler J, Stoppelmann G (2000) Polymer 42:1095
2. Cho JW, Paul DR (2001) Polymer 42:1083
3. Wang Y, Zhang L, Tang C, Yu D (2000) J Appl Polym Sci 78:1878
4. Fu X, Qutubuddin S (2001) Polymer 42:807
5. Petrovicova R, Knight R, Schadler LS, Twardowski TE (2000) J Appl Polym Sci 78:2272
6. Petrovic ZS, Javni I, Waddon A, Banhegi G (2000) J Appl Polym Sci 76:133
7. Rong MZ, Zhang MQ, Zheng YX, Zeng HM, Walter R, Friedrich K (2001) Polymer 42:167
8. Rong MZ, Zhang MQ, Zheng YX, Zeng HM, Walter R, Friedrich K (2001) Polymer 42:3301
9. Hasegawa N, Okamoto H, Kato M, Usuki A (2000) J Appl Polym Sci 78:1918
10. Levita G, Marchetti A, Lazzari A (1989) Polym Eng Sci 19:39
11. Kinloch AJ, Taylor AC (2006) J Mater Sci 41:3271. doi: [10.1007/s10853-005-5472-0](https://doi.org/10.1007/s10853-005-5472-0)
12. Sumita M, Shizuma T, Miyasaka K, Ishikawa K (1983) J Macromol Sci B 22:601
13. Sumita M, Tsukumo Y, Shizuma T, Miyasaka K, Ishikawa K (1983) J Mater Sci 18:1758. doi: [10.1007/BF00542072](https://doi.org/10.1007/BF00542072)
14. Li L, Zou H, Shao L, Wang G, Chen J (2005) J Mater Sci 40:1297. doi: [10.1007/s10853-005-6956-7](https://doi.org/10.1007/s10853-005-6956-7)
15. Kopczynska A, Ehrenstein GW (2007) J Mater Educ 29:325
16. Che J, Xiao Y, Luan B, Dong X, Wang X (2007) J Mater Sci 42:4967. doi: [10.1007/s10853-006-0537-2](https://doi.org/10.1007/s10853-006-0537-2)
17. Brostow W, Chonkaew W, Datashvili T, Menard KP (2009) J Nanosci Nanotechnol 9:1916
18. Bermudez M-D, Brostow W, Carrion-Vilches FJ, Sanes J (2010) J Nanosci Nanotechnol 10:6683
19. Kleinwechter H, Janzen C, Knipping J, Wiggers H, Roth P (2002) J Mater Sci 37:4349. doi: [10.1023/A:1020656620050](https://doi.org/10.1023/A:1020656620050)
20. Viguera-Santiago E, Hernandez-Lopez S, Brostow W, Olea-Mejia O, Lara-Sanjuan O (2010) e-Polymers no. 100
21. Nogales A, Broza G, Roslanic Z, Schulte K, Sics I, Hsiao BS, Sanz A, Garcia Gutierrez MC, Rueda DR, Domingo C, Ezquerra TA (2004) Macromolecules 37:7669
22. Broza G, Schulte K (2008) Polym Eng Sci 48:2033
23. Giraldo LF, Brostow W, Devaux E, Lopez BL, Perez LD (2008) J Nanosci Nanotechnol 8:3176
24. Dos Santos DS Jr, Goulet PJG, Pieczonka NPW, Oliveira ON Jr, Aroca JR (2004) Langmuir 20:10273
25. Olea-Mejia O, Brostow W, Buchman E (2010) J Nanosci Nanotechnol 10:8524
26. Morrell R (1985) Handbook of properties of technical and engineering ceramics. Part I: An introduction for the engineering designer her majesty's stationary office England 82
27. Gleiter H (2000) Acta Mater 48:1
28. Burn RB (1982) Polyester molding compounds. Marcel Dekker, New York
29. Hietalathi K, Root A, Skeifvars M, Sundholm F (1997) J Appl Polym Sci 65:77

30. Martuscelli E, Musto P, Ragosta G, Scarinzi G, Bertotti E (1993) *J Polym Sci B* 31:619
31. Bellenger V, Mortaigne D, Grenier-Loustalot MF, Verdu J (1992) *J Appl Polym Sci* 44:643
32. Chen JS, Yu TL (1998) *J Appl Polym Sci* 69:871
33. Yang YS, Pascault JP (1997) *J Appl Polym Sci* 64:133
34. Yang YS, Pascault JP (1997) *J Appl Polym Sci* 64:147
35. Menard KP (2008) Dynamic mechanical analysis—an introduction, 2nd edn. CRC press, Boca Raton, FL
36. Chan CM, Wu J, Li JX, Cheung YK (2002) *Polymer* 43:2981–2992
37. Li H, Yan Y, Liu B, Chen W, Chen S (2007) *Powder Technol* 178:203–207
38. Shang SW, Willams JW, Soderholm KJM (1994) *J Mater Sci* 29:2406. doi:[10.1007/BF00363434](https://doi.org/10.1007/BF00363434)
39. Zhang J, Wang X, Lu L, Li D, Yang X (2003) *J Appl Polym Sci* 87:381–385
40. Chen N, Wan C, Zhang Y (2004) *Polym Test* 23:169–174
41. Li HB (1999) *Shanghai Chem* 8:4
42. Noor Ahmad F, Jaafar M, Palaniandy S, Mohd Azizi KA (2008) *Compos Sci Technol* 68:346–353
43. Nakagawa H, Sano H (1992) *Polym Chem* 26:249
44. Mareri P, Bastide S, Binda N, Crespy A (1988) *Compos Sci Technol* 58:747
45. Cao YM, Sun J, Yu DH (2002) *J Appl Polym Sci* 83:70–77
46. Rouli-Moloney AC, Cantwell WJ, Kaush HH (1987) *Polym Compos* 8:314
47. Li F, Ge J, Honigfort PS (1999) *Polymer* 40:4987
48. Al-Kandary Sh, Ali AM, Ahmad Z (2005) *J Appl Polym Sci* 98:2521
49. Lu H, Xu X, Li X, Zhang Z (2006) *Bull Mater Sci* 29:485–490
50. Xie XL, Liu QX, Yiu Li, Mai YW (2004) *Polymer* 45:6665–6673
51. Jin FN, Park SN (2009) *Bull Korean Chem Soc* 30:2
52. Brostow W, Hagg Lobland HE, Narkis M (2006) *J Mater Res* 21:2422
53. Brostow W, Hagg Lobland HE (2010) *J Mater Sci* 45:242. doi:[10.1007/s10853-009-3926-5](https://doi.org/10.1007/s10853-009-3926-5)
54. Yasmin A, Isaac MD (2004) *Polymer* 45:8211–8219